

Journal of Biomedical Optics

SPIEDigitalLibrary.org/jbo

Single-shot speckle noise reduction by interleaved optical coherence tomography

Lian Duan
Hee Yoon Lee
Gary Lee
Monica Agrawal
Gennifer T. Smith
Audrey K. Ellerbee

Single-shot speckle noise reduction by interleaved optical coherence tomography

Lian Duan, Hee Yoon Lee, Gary Lee, Monica Agrawal, Gennifer T. Smith, and Audrey K. Ellerbee*
Stanford University, E.L. Ginzton Laboratory and Department of Electrical Engineering, Stanford, California 94305, United States

Abstract. Speckle noise is one of the dominant factors that degrade image quality in optical coherence tomography (OCT). Here, we propose a new strategy, interleaved OCT (iOCT), for spatial compounding and angular compounding. We demonstrate the efficiency of compounding with iOCT to restrain speckle noise without compromising imaging speed in phantoms and tissue samples. © 2014 Society of Photo-Optical Instrumentation Engineers (SPIE) [DOI: 10.1117/JBO.19.12.120501]

Keywords: optical coherence tomography; speckle reduction; angular compounding; spatial compounding.

Paper 140648LR received Oct. 6, 2014; accepted for publication Nov. 19, 2014; published online Dec. 8, 2014.

The appearance of speckle is inherent to coherent imaging techniques such as optical coherence tomography (OCT).¹ Although speckle is known to sometimes carry information about the type and distribution of microstructures, it is primarily treated as a source of noise in OCT images since it reduces image resolution and blurs structural boundaries. Many techniques have been proposed to restrain speckle in OCT using either postprocessing (e.g., digital filters,² wavelet transforms,³ fractional Fourier domains⁴) or compounding approaches (e.g., spatial,⁵ angular,^{6,7} strain,⁸ or frequency compounding^{9,10}). Although postprocessing methods can effectively reduce speckle noise, they often suffer from high computational costs or reduce axial resolution. Hardware-based compounding techniques preserve small structural information and are more computationally efficient; however, they usually require complicated optical setups and multiple acquisitions.⁵⁻⁹ In this work, we introduce a new strategy for hardware-based spatial and angular compounding based on interleaved OCT (iOCT).^{11,12} Compared to other techniques, iOCT acquires decorrelated speckle patterns simultaneously, thereby achieving speckle suppression without compromising imaging speed.

The general method of iOCT has been described elsewhere.^{11,12} In brief, an optical multibeam demultiplexor, such as a virtually imaged phased array (VIPA),¹³ is inserted into the sample arm of a broadband, swept-source (SS) OCT system to produce line illumination. Interleaved frequency combs comprising different sets of wavelengths exit the VIPA spatially separated and travel to different lateral points at the imaging plane.

Hence, the interferograms for different lateral points are spectrally encoded.

The iOCT system engine we used,¹² shown in Fig. 1, consisted of a home-built SS-OCT system centered at 1310 nm with a full-width-at-half-maximum bandwidth of 100 nm, a sweep rate of 200 kHz and a coherence length of >50 mm. A home-made, air-spaced VIPA (thickness = 3.7 mm) comprising a D-shaped mirror and silver-coated optical flat (transmissivity = 23.3%) was utilized to generate seven interleaved frequency combs. The axial resolution of the system was 16 μm in air. The ranging depth of the system was 1.91 mm for frequency combs comprising 480 wavelengths. The output power of the light source was 27.6 mW, with 3.4 mW illuminating the sample, and the sensitivity of the system, which was limited by the number of points in the A-scan,¹² was 83 dB. The digitizer could collect up to 4096 points at a rate of 1.2 GS/s within each sweep period.

Spatial compounding combines speckle patterns from laterally adjacent points to generate a speckle-reduced A-scan at a single location. The iOCT configuration described in previous work,¹² which measures A-scans from different lateral points, could directly implement spatial compounding [Fig. 1(b)]. In this configuration, a cylindrical lens ($f = 200$ mm) was incident on the VIPA. In one dimension, the illumination pattern on the sample was a line; in the other dimension, it was a focused spot. The gradient of colors used in Fig. 1(b) illustrates how different lateral positions are illuminated by different frequency combs.

The loss of lateral resolution in the direction of the line illumination caused by spatial compounding makes angular compounding an attractive alternative for speckle repression.^{6,7} Angular compounding preserves lateral resolution because it operates by illuminating a single sample point from multiple directions. To perform angular compounding, the cylindrical lens in the iOCT setup was replaced by a spherical lens ($f = 200$ mm), as shown in Fig. 1(c), yielding a conical beam input to the VIPA. In this configuration, the VIPA generates multiple frequency combs that propagate toward the sample at different directions. The objective lens focuses all combs to a single spot on the sample, causing each frequency comb, represented by a different color, to illuminate the sample spot at a unique angle.

iOCT interferograms were processed as previously described to yield distinct B-scans for each illumination condition.¹¹ To achieve speckle reduction, A-scans from different frequency combs were combined via intensity averaging.⁵ To characterize the degree of speckle contained in the OCT image, the speckle contrast (SC) parameter was calculated as defined by Goodman.¹⁴ The speckle contrast ratio (SCR) was then calculated as the ratio of the SC between images with and without speckle reduction and used to compare the effectiveness of speckle reduction.

We fabricated a five-layer, scattering polydimethylsiloxane phantom (Sylgard 184 Silicone Elastomer, Dow/Corning) comprising titanium dioxide powder particles (TiO₂ anatase, 232022, Sigma-Aldrich) with an average size of 130 ± 70 nm. The five layers were produced by spin-coating and were ordered from top to bottom to yield a pattern of high-high-low-high-high scattering with a thickness ordering of 150-150-100-100-100 μm .

The setup for spatial compounding utilized a 60-mm objective lens to focus OCT beams on the sample, yielding a 79- μm

*Address all correspondence to: Audrey K. Ellerbee, E-mail: audrey@ee.stanford.edu

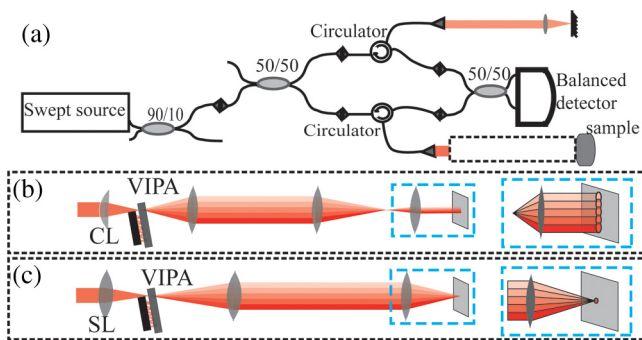


Fig. 1 System schematic of a line-scan interleaved optical coherence tomography (iOCT) setup (a) and its sample arm design for spatial compounding (b) and angular compounding (c). CL: cylindrical lens. SL: spherical lens.

lateral line length and an 11- μm lateral resolution. Figures 2(a) and 2(b) compare phantom images of a single iOCT image (used as a surrogate for a traditional OCT image) and the average of seven iOCT images that underwent spatial compounding using a VIPA with a spectral resolution of 56.7 pm. The measured SCs were 2.27 and 1.31 in the areas marked by white rectangles, respectively. It is clear that spatial compounding effectively reduced speckle (SCR = 0.58). The yellow arrows in the image serve to highlight layers that are better delineated in the speckle-reduced image than the original image.

The elevated value of the obtained SC compared to theory ($1/\sqrt{7}$) is possibly due to the unevenly distributed power for each frequency comb and limitations from the spectral resolution of the VIPA,⁵ which can affect the correlation between adjacent frequency combs and decrease the efficiency of speckle reduction. To better understand the effect of the VIPA spectral resolution on the SC, the black line in Fig. 3 shows the SCR as a function of the spectral resolution of the VIPA. The spectral resolution was controlled by varying the tilt angle of the second surface of the VIPA (i.e., the D-shaped mirror). Given that a low SCR suggests a good performance, it is clear from this graph that the speckle reduction efficiency degrades as the spectral resolution of the VIPA decreases.

The setup for angular compounding utilized a 30-mm objective lens to focus the light to a spot on the sample. In this way, we collected seven simultaneous B-scans, each with a different illumination angle. Figures 2(c) and 2(d) show a

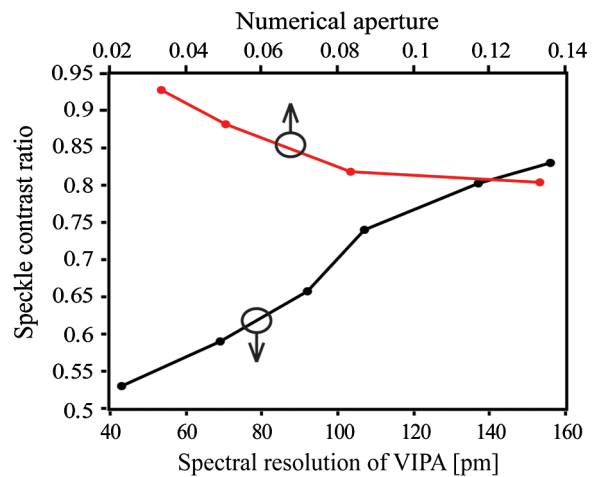


Fig. 3 Speckle contrast ratio (SCR) versus spectral resolution of the VIPA (black line) in spatial compounding and versus numerical aperture (NA) in angular compounding (red line). Arrows indicate lateral axes applied to the curves.

single iOCT B-scan and a B-scan generated from angular compounding. In this measurement, we used a 250-mm focal length lens immediately following the VIPA to achieve a numerical aperture (NA) of 0.083. The measured SCs were 1.31 and 1.05 in the areas noted by white rectangles in Figs. 2(c) and 2(d), respectively, yielding an SCR of 0.80. The improved speckle with angular compounding is evident.

To understand how the range of angles included in the averaging affects the compounding result, we evaluated the speckle reduction achieved for different NAs of light exiting the iOCT system by varying the focal length of the lens placed after the VIPA ($f = 100$ to 400 mm). The red curve in Fig. 3 shows the measured SCR with/without speckle reduction in iOCT by systems with different NAs. As the NA increases, better speckle reduction efficiency can be achieved. Nevertheless, the SCs achievable with angular compounding were generally worse than those possible with spatial compounding. We hypothesize that this may be due to the high correlation of structure-determined speckle patterns in the region of overlap.

To verify the ability of iOCT-based speckle reduction to work with biomedical samples, we imaged samples of a porcine bladder. B-scan images consisting of 850 A-lines were taken from fresh *ex-vivo* porcine bladder over an imaging range of 4 and

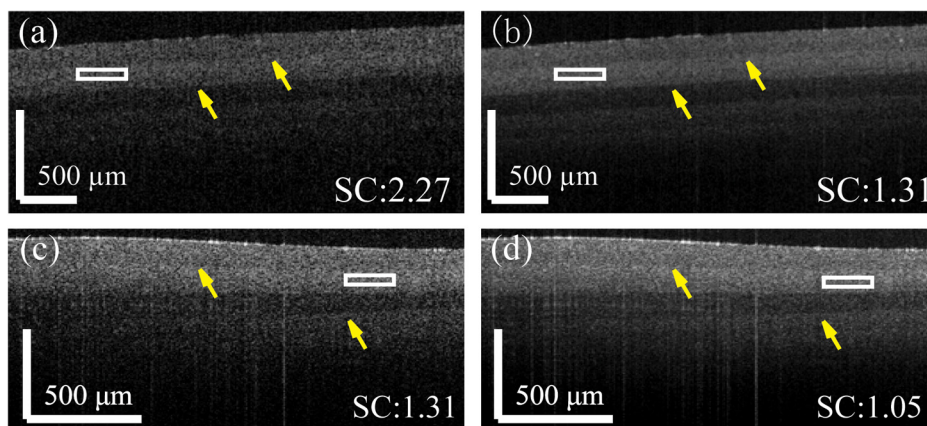


Fig. 2 Comparison of phantom images before (a and c) and after (b and d) speckle reduction by spatial compounding (a and b) and angular compounding (c and d). SC: speckle contrast.

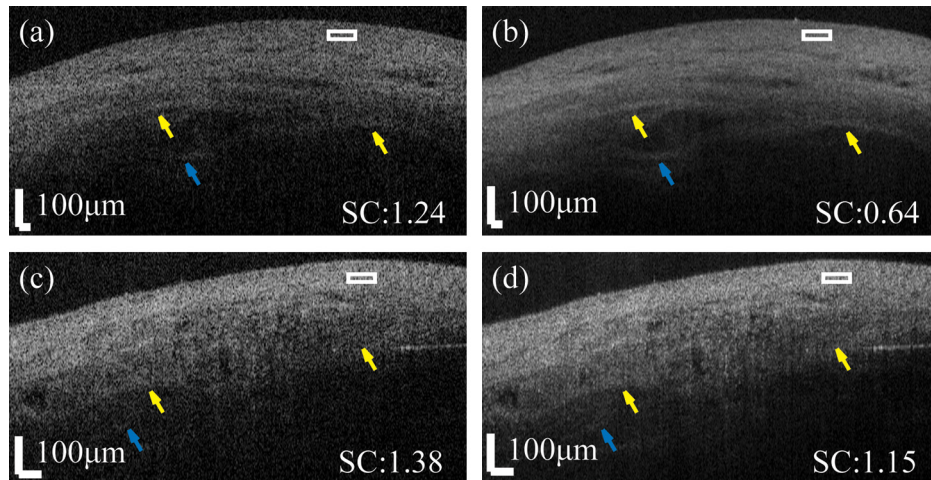


Fig. 4 Single and speckle-reduced iOCT images of *ex vivo* porcine bladder imaged by spatial compounding (a and b) and angular compounding (c and d) iOCT.

2 mm by spatial compounding and angular compounding iOCT systems, respectively.

In the spatial compounding iOCT measurement, we optimized the spectral resolution of the VIPA to 43 pm. Figures 4(a) and 4(b) show images before and after speckle reduction. The smooth appearance of the lamina propria layer in Fig. 4(b) contrasts with the grainy appearance of a single iOCT image [Fig. 4(a)]. The SC evaluated in the visually homogeneous area marked by the rectangles in these two images was calculated to be 1.24 and 0.64, respectively, yielding an SCR of 0.52. The speckle-reduced iOCT image also shows a clearer boundary between the lamina propria and the muscularis propria as indicated by yellow arrows, as well as enhanced visibility of the structure in the muscularis propria, as indicated by blue arrows.

We also performed angular compounding on similar bladder samples using an NA of 0.083. Figures 4(c) and 4(d) show single iOCT and speckle-reduced iOCT images, respectively. The measured SCs in the small area denoted by the white rectangles were 1.38 and 1.15, respectively, leading to an SCR of 0.83. Similar to the spatial compounding results, the speckle-reduced image shows a more distinct layer structure in the region of the lamina propria. In addition, the noisy pattern visible in the muscularis propria in Fig. 4(c) is replaced by more visible muscle structures in Fig. 4(d), as indicated by blue arrows.

In this letter, we present the first demonstration of single-shot spatial compounding for speckle reduction without compromising the imaging speed. By using a spherical lens input to the VIPA, we also demonstrated a novel configuration for iOCT that can implement single-shot angular compounding. Both spatial and angular compounding with iOCT was shown to achieve good speckle reduction and neither required mechanically scanning parts. The simplicity of the iOCT design and the single-shot nature of the technique can make iOCT a viable strategy for speckle-free imaging *in vivo*.

Acknowledgments

We acknowledge the help of Tahereh Marvdashti for useful discussions. Lian Duan was funded by a Stanford Bio-X Seed Grant. Gary Lee was funded by a scholarship from the

Agency for Science, Technology and Research, Singapore. Monica Agrawal was supported by the Electrical Engineering Research Experience for Undergrads program in Stanford University. Gennifer Smith was funded by an NSF graduate research fellowship.

References

1. J. M. Schmitt, S. H. Xiang, and K. M. Yung, "Speckle in optical coherence tomography," *J. Biomed. Opt.* **4**(1), 95–105 (1999).
2. A. Ozcan et al., "Speckle reduction in optical coherence tomography images using digital filtering," *J. Opt. Soc. Am. A* **24**, 1901–1910 (2007).
3. J. Xu et al., "Wavelet domain compounding for speckle reduction in optical coherence tomography," *J. Biomed. Opt.* **18**(9), 096002 (2013).
4. N. Lippok, P. Nielsen, and F. Vanholsbeeck, "Single-shot speckle reduction and dispersion compensation in optical coherence tomography by compounding fractional fourier domains," *Opt. Lett.* **38**(11), 1787–1789 (2013).
5. M. Szkulmowski et al., "Efficient reduction of speckle noise in optical coherence tomography," *Opt. Express* **20**, 1337–1359 (2012).
6. A. E. Desjardins et al., "Angle-resolved optical coherence tomography with sequential angular selectivity for speckle reduction," *Opt. Express* **15**, 6200–6209 (2007).
7. H. Wang and A. M. Rollins, "Speckle reduction in optical coherence tomography using angular compounding by b-scan doppler-shift encoding," *J. Biomed. Opt.* **14**(3), 030512 (2009).
8. B. F. Kennedy et al., "Speckle reduction in optical coherence tomography by strain compounding," *Opt. Express* **35**(14), 2445–2447 (2010).
9. M. Pircher et al., "Speckle reduction in optical coherence tomography by frequency compounding," *J. Biomed. Opt.* **8**(3), 565–569 (2003).
10. G. van Soest et al., "Frequency domain multiplexing for speckle reduction in optical coherence tomography," *J. Biomed. Opt.* **17**(7), 076018 (2012).
11. H. Y. Lee et al., "Interleaved optical coherence tomography," *Opt. Express* **21**, 26542–26556 (2013).
12. H. Y. Lee et al., "Scalable multiplexing for parallel imaging with interleaved optical coherence tomography," *Biomed. Opt. Express* **5**, 3192–3203 (2014).
13. M. Shirasaki, "Large angular dispersion by a virtually imaged phased array and its application to a wavelength demultiplexer," *Opt. Lett.* **21**, 366–368 (1996).
14. J. W. Goodman, *Statistical Optics*, Wiley, New York (1985).